

## Importance of the Nuclear Density Distribution on Pre-equilibrium Decay

Marshall Blann

*Department of Chemistry and Nuclear Structure Laboratory, University of Rochester, Rochester, New York 14627*  
(Received 13 January 1972)

A Thomas-Fermi approach is used to investigate the importance of the nuclear density distribution on pre-equilibrium decay. Two different density-dependent phenomena are pointed out, and both are shown to be equally important in modifying and improving pre-equilibrium decay predictions with respect to earlier models in which average density distributions were assumed.

Several articles recently published have dealt with the topic of calculating the absolute spectral yields of particles emitted in nuclear reactions prior to the attainment of statistical equilibrium. One is the approach of Harp, Miller, and Berne, in which a set of coupled differential equations is solved for the competition between particle emission and the spreading to more complex states.<sup>1,2</sup> The second approach has been called the hybrid model,<sup>3</sup> and is an extension of the exciton model due to Griffin,<sup>4-6</sup> in which excitation is assumed to spread by a series of two-body interactions, with probabilities characterized by intermediate-state density expressions. Both models are based on phase-space arguments, with internal transition rates based on nucleon-nucleon scattering cross sections and on the average nuclear density.<sup>1-3</sup> Both models give incorrect cross sections and spectral distributions when applied to nucleon-induced reactions at medium energies.<sup>2,7</sup>

In this paper a crude model is presented which illustrates the significance and consequences of the nuclear density distribution in resolving the

discrepancies noted above. This will be done in terms of reformulating the hybrid model with a geometry dependence based on the impact parameters for the partial waves initiating the reaction. It will be assumed that the reaction initiated by each partial wave proceeds in the spherical shell-shaped region of thickness  $\lambda/2\pi$  with radius defined by the initial impact parameter. This neglects the spherical geometry of the problem, and the diffusion of excited particles and holes between these regions as the equilibration process proceeds. Since the first interaction is the most important with respect to the decay channel, the second approximation above becomes poorer as the contribution to the decay spectrum becomes progressively smaller, and so may not be so unreasonable. The neglect of the spherical geometry amounts to the assumption that the forward projection of the interaction is the important consideration in the initial interaction, and that the higher impact parameters are most important.

The hybrid model<sup>3</sup> predicts the probability of emission of a particle of type  $\nu$  in the channel energy range  $\epsilon$  to  $\epsilon + d\epsilon$  as

$$P(\epsilon) d\epsilon = \sum_{\substack{n=n_0 \\ \Delta n = +2}}^{\infty} {}_n P_{\nu} [N_n(\epsilon, U)/N_n(E)] g d\epsilon \{ \lambda_c(\epsilon) / [\lambda_c(\epsilon) + \lambda_{n+2}(\epsilon)] \} D_n, \quad (1)$$

where  ${}_n P_{\nu}$  is the number of particles of type  $\nu$  in an  $n$ -exciton state.  $N_n(\epsilon, U)$  is the number of ways  $n$  excitons can be arranged such that one exciton, if emitted, would have channel energy  $\epsilon$ , leaving a residual excitation of  $U = E - B_{\nu} - \epsilon$  distributed between the other  $n - 1$  excitons. The quantity  $N_n(E)$  represents the total number of combinations of  $n$  particles plus holes at excitation  $E$ . The quantity in the first set of square brackets represents the fraction of the  $n$ -exciton states having one exciton at energy  $\epsilon$  with respect to the continuum. The limiting value of the emission probability as defined by Eq. (1), integrated over all particle emission energy for decay of a particular state with  ${}_n P_{\nu}$  particles, is not unity but  ${}_n P_{\nu}$ , i.e., the total number of excited particles.

Also in Eq. (1), the emission rate into the continuum  $\lambda_c(\epsilon)$  of a particle at excitation  $\epsilon$  is given by

$$\lambda_c(\epsilon) = \sigma_{\nu} v \rho_c / g_{\nu} V, \quad (2)$$

where  $\sigma_{\nu}$  is the inverse cross section and  $v$  the velocity of the particle having a density of states  $\rho_c$  in the continuum, and a single-particle density of states  $g_{\nu}$  in the nucleus.  $V$  is an arbitrary volume, canceled by the same volume in  $\rho_c$ .

The internal transition rate  $\lambda_{n+2}(\epsilon)$  of an excited particle at energy  $\epsilon + B_{\nu}$  above the Fermi energy has

been based on calculated mean free paths in nuclear matter<sup>8</sup> and for energies below 100 MeV may be represented as

$$\lambda_{n+2}(\epsilon) = [1.4 \times 10^{21}(\epsilon + B_n) - 6 \times 10^{19}(\epsilon + B_n)^2] / k \text{ sec}^{-1}, \quad (3)$$

where a value of  $k=1$  gives the result for nuclear matter of average interior density, which will be represented as  $\bar{d}$ . The  $D_n$  in (1) is simply a prior decay depletion factor.<sup>3</sup>

Equation (1) may now be expressed as a cross section for particle emission summed over the reaction zones referred to above,

$$\sigma(\epsilon) d\epsilon = \pi \left( \frac{\lambda}{2\pi} \right) \sum_{l=0}^{\infty} (2l+1) T_l P(\epsilon) d\epsilon, \quad (4)$$

where the transmission coefficients  $T_l$  are for the projectile and, in the examples to be presented in this work, have been taken from the nuclear optical model, as have the inverse cross sections of Eq. (2).<sup>9</sup>

The  $T_l$  in Eq. (4) serve only to give the cross section of interaction for the projectile within the zone defined by  $l\hbar$  units of angular momentum;

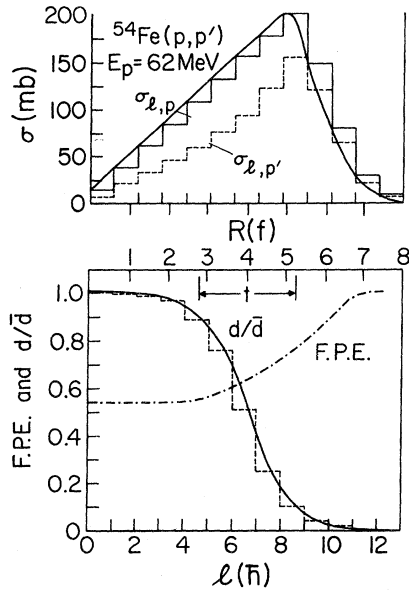


FIG. 1. The lower half of the figure gives the ratio of nuclear density at radius  $R$  (upper abscissa) to the interior density  $\bar{d}$ , shown as a continuous solid curve, for a mass-55 nucleus. The dashed histogram shows the average density ratios used in each reaction zone defined by the partial wave  $l$  (lower abscissa). The 90–100% skin thickness  $t$  is also indicated. The fraction pre-equilibrium emission predicted for each zone is shown as a smooth dot-dashed curve. The upper curves show histograms for the total reaction cross section of each zone, and the corresponding integrated pre-equilibrium proton emission cross sections.

the dissipation of excitation in the exit channel is a separate question, although both entrance and exit channels are influenced by the density distribution.

It will be assumed, consistent with electron scattering data, that the nuclear density is given by a Fermi distribution,<sup>10</sup>

$$d(R) = \bar{d} [\exp(R - c) / Z + 1]^{-1}, \quad (5)$$

where  $d(R)$  is the density at radius  $R$ ,  $c = 1.07A^{1/3}$  fm, and  $Z = 0.55$  fm. This distribution is illustrated in Fig. 1 for an  $A = 55$  nucleus. The nuclear density can influence the pre-equilibrium decay spectrum given by Eq. (4) in two ways.

The more obvious is an increase in the mean free path for nucleon-nucleon collisions, increasing the particle emission probability by decreasing the rate of “spreading.” This will be treated here by defining  $k$  of Eq. (3) as

$$k = k(d) = \bar{d} / \langle d(R) \rangle, \quad (6)$$

where  $\langle d(R) \rangle$  represents the average density in the disk of radius  $l\lambda/2\pi$  to  $(l+1)\lambda/2\pi$ .

A second, and it will be shown equally important, consequence of the density distribution is the changing of the potential well depth in the region of interest, in the sense of the Thomas-Fermi model.<sup>11</sup>

This in turn has two consequences, the more important of which is limiting the depth of the hole degree of freedom, and therefore the combinatorial probabilities of Eq. (1). The second effect, less important and in the opposite direction, is the modifying of the single-particle level density  $g_n$  of Eq. (2), which now also becomes a function of the density. The usual state density expressions used in both pre-equilibrium and equilibrium statistical analyses assume that infinitely deep hole states are possible, and this assumption may lead to very serious errors in both cases when the average excitation per particle or hole is a significant fraction of the potential well depth.

The potential depth, measured with respect to the Fermi energy, will be taken in each reaction zone as

$$V(R) = 40[\langle d(R) \rangle / \bar{d}]^{2/3} \text{ MeV}, \quad (7)$$

and the single-particle density of states will be

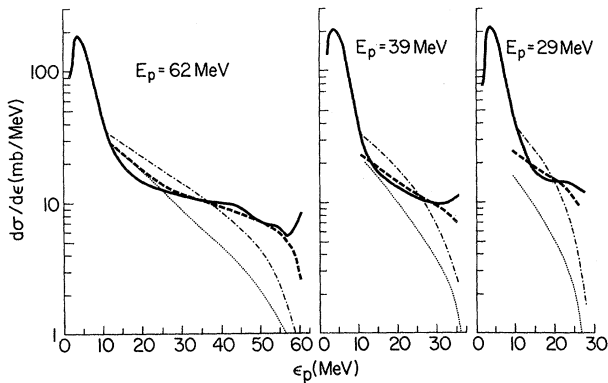


FIG. 2. Calculated and experimental  $(p, p')$  spectra on an  $^{54}\text{Fe}$  target for incident proton energies of 62, 39, and 29 MeV. Experimental results (Ref. 13) are represented by the heavy solid curves. Calculated pre-equilibrium components are based on the hybrid model (dotted curve), and on the density-dependent models under discussion in this work. The dot-dashed curve shows the effect of including a density-dependent mean free path. The dashed curve represents the effect of also including the density-dependent potential.

taken as

$$g_\nu = g_\nu(R) = [40/V(R)]A/28, \quad (8)$$

where  $A$  is the mass number of the excited nucleus. In calculations to be presented, combinatorial probabilities considering the finite well depth have been used only for decay of the first excited state, which is by far the most important point of application. With  $g = g_n + g_p$ , these values are

$$N_{2p-1h}(\epsilon, U) = \frac{1}{2}gV(R), \quad U > V(R) \quad (9)$$

$$N_{2p-1h}(E) = \frac{1}{4}g^2V(R)[2E - V(R)], \quad E > V(R).$$

Values identical to those given by Ericson's intermediate-state density expressions (divided by  $g$ ) were used in all other cases.<sup>12</sup>

Bertrand and Peelle have measured  $(p, p')$  spectra on a broad range of targets for incident proton energies of 29 to 62 MeV.<sup>13</sup> One such target is  $^{54}\text{Fe}$ , which has been used to illustrate the points of this article. The high-energy or pre-equilibrium components of the spectra from targets of  $^{27}\text{Al}$  to  $^{209}\text{Bi}$  from Ref. 13 are all generally similar, and so this system is representative. Results are shown in Fig. 2. The results of the hybrid model are shown for the spectrum expected from a reaction starting with a  $2p-1h$  initial state; the incorrect spectra distributions and cross sections are obvious. The effect of repeating the calculation with  $k$  of Eq. (6) substituted into (3) [but not using the state densities of (8) and (9)] is also shown. An increase in cross

sections results, still giving an incorrect spectral distribution, too low cross sections at high channel energies, and too high cross sections at lower channel energies. Finally the calculations are presented including the potential depth restriction of Eqs. (8) and (9), which for lack of a better name will be called the geometry-dependent hybrid model. The agreement with the experimental spectrum is surprisingly good, and illustrates the importance of the nuclear matter density effects discussed on the pre-equilibrium spectrum. These effects are further illustrated in Fig. 1 where the predicted radial dependence of pre-equilibrium emission is indicated. No attempt was made in the calculations of Fig. 2 to reproduce the equilibrium spectral component.

Many of the approximations made in this Thomas-Fermi approach to the pre-equilibrium decay problem could be improved upon. Average densities could be calculated with three-dimensional geometry; average potentials in the reaction zones could be computed rather than potentials at average zone densities. An equally important change would be use of a Fermi-gas single-particle density  $g$ , rather than extrapolating a constant value over such a wide range of excitation. These changes would increase the effects under discussion and should in fact give slightly better agreement with the experimental data. The goal of this work is, however, to illustrate, as simply as possible, the importance of the density effects noted, as illustrated in Figs. 1 and 2.

<sup>1</sup>G. D. Harp, J. M. Miller, and B. J. Berne, *Phys. Rev.* **165**, 1166 (1968).

<sup>2</sup>G. D. Harp and J. M. Miller, *Phys. Rev. C* **3**, 1847 (1971).

<sup>3</sup>M. Blann, *Phys. Rev. Lett.* **27**, 337, 700(E), 1550(E) (1971).

<sup>4</sup>J. J. Griffin, *Phys. Rev. Lett.* **17**, 478 (1966).

<sup>5</sup>J. J. Griffin, *Phys. Lett.* **24B**, 5 (1967).

<sup>6</sup>J. J. Griffin, in *Nuclear Physics: an International Conference*, edited by R. L. Becker (Academic, New York, 1967), p. 778.

<sup>7</sup>M. Blann and A. Mignerey, to be published.

<sup>8</sup>K. Kikuchi and M. Kawai, *Nuclear Matter and Nuclear Reactions* (North-Holland, Amsterdam, 1968).

<sup>9</sup>G. S. Mani, M. A. Melkanoff, and I. Iori, Centre d'Etudes Nucléaires de Saclay Report No. CEA 2379, 1963 (unpublished).

<sup>10</sup>R. Hofstadter, *Annu. Rev. Nucl. Sci.* **7**, 295 (1957).

<sup>11</sup>W. D. Myers, *Ann. Phys. (New York)* **55**, 395 (1969).

<sup>12</sup>T. Ericson, *Advan. Phys.* **9**, 425 (1960).

<sup>13</sup>F. E. Bertrand and R. W. Peelle, ORNL Reports No. 4274, 1968, No. 4450, No. 4455, No. 4456, 1969, No. 4471, No. 4469, 1970, No. 4628, 1971 (unpublished).